Research article

Bi-directional Modulation of Hyperpolarization-Activated Cation Currents (I_h) by Ethanol in Rat Hippocampal CA3 Pyramidal Neurons

Valentina Licheri[a]*, Giuseppe Talani[b], Giovanni Biggio[a,b], and Enrico Sanna[a,b]

[a]Department of Life and Environmental Sciences, Section of Neuroscience and Anthropology, University of Cagliari, Monserrato, Italy. [b]Institute of Neuroscience, National Research Council (CNR), Cittadella Universitaria di Monserrato, S.P. 8, km 0,700, 09042 Monserrato (CA), Italy.

Running title: Ethanol modulation of I_h in CA3 pyramidal neurons

Corresponding author: Enrico Sanna, Department of Life and Environmental Sciences, Section of Neuroscience and Anthropology, University of Cagliari, and Institute of Neuroscience, National Research Council (CNR), Cittadella Universitaria di Monserrato, S.P. 8, km 0,700, 09042 Monserrato, Cagliari (Italy).

*Present address: Department of Neurosciences, University of New Mexico School of Medicine, Albuquerque, NM, U.S.A.

Highlights

- HCN channels regulate synaptic signaling, firing discharge, and membrane excitability.
- EtOH bi-directionally modulate the function of HCN in rat CA3 pyramidal neurons.
- Lower (20 mM) concentrations of EtOH enhance and higher (80 mM) reduce HCN-mediated I_h.
- Modulation of I_h by EtOH is mimicked by forskolin and antagonized by drugs that interfere with the AC/cAMP/PKA intracellular pathway.
- These data support the notion that HCN represent an important molecular target through which EtOH may alter neuronal activity.

Abstract

It is widely acknowledged that ethanol (EtOH) can alter many neuronal functions, including synaptic signaling, firing discharge, and membrane excitability, through its interaction with multiple membrane proteins and intracellular pathways. Recently, it has been demonstrated that EtOH enhances the firing rate of hippocampal GABAergic interneurons and thus the presynaptic GABA release at CA1 and CA3 inhibitory synapses through a positive modulation of the hyperpolarization-activated cyclic nucleotide-gated cation channels (HCN). Activation of HCN produce an inward current, commonly called I_h, which plays an essential role in generating/regulating specific neuronal activities in GABAergic interneurons and principal glutamatergic pyramidal neurons such as those in the CA3 subregion. Since the direct effect of EtOH on HCN expressed in CA3 pyramidal neurons was not thoroughly elucidated, we investigated the possible interaction between EtOH and HCN and the impact on excitability and postsynaptic integration of these neurons. Patch-clamp recordings were performed in single CA3 pyramidal neurons from acute male rat coronal hippocampal slices. Our results show that EtOH modulates HCN-mediated I_h in a concentration-dependent and bi-directional manner, with a positive modulation at lower (20 mM) and an inhibitory action at higher (70-80 mM) concentrations. The modulation of I_h by EtOH was mimicked by forskolin and antagonized by different drugs that selectively interfere with the AC/cAMP/PKA intracellular pathway. Altogether, these data further support the evidence that HCN may represent an important molecular target through which EtOH may regulate neuronal activity.

Keywords: HCN, I_h, ethanol, CA3 pyramidal neurons, rat hippocampus

1. Introduction

Ethanol (EtOH) is among the most widely consumed drugs of abuse. It can produce a complex array of neurobiological effects resulting in marked behavioral alterations in humans and laboratory

60 animals (Abrahaho et al., 2017). The actions of EtOH are time- and dose-dependent, and, following
61 its acute exposure, they may range from euphoria and mild stimulation to sedation, motor
62 incoordination, and cognitive impairment (Diamond and Messing, 1994; Zorumski et al., 2014; Van
63 Skike et al., 2019). Although the mechanisms underlying ethanol's actions are not fully understood,
64 it is believed that they might result from its capacity to interact directly and indirectly with multiple
65 molecular targets in the central nervous system (CNS). These include neuronal membrane proteins
66 such as ligand- and voltage-gated ion channels and intracellular signaling proteins which play relevant
67 roles in neuronal physiology and synaptic transmission (Harris et al., 2008; Abrahaho et al., 2017;
68 Egervari et al., 2021).
69 Recently, the hyperpolarization-activated and cyclic nucleotide-gated channels (HCN) have been
70 suggested as a potential new molecular target for EtOH action in rodents (Tateno and Robinson, 2011)
71 and humans (Chen et al., 2012).
72 HCN activation mediates the so-called hyperpolarization-activated current (I_h), which was first
73 discovered in the sinoatrial node tissue (Noma and Irisawa, 1976), where it was named "funny
74 current" (I_f); thereafter, a similar I_h was characterized in rod photoreceptors and hippocampal
75 pyramidal neurons (Bader et al., 1979; Halliwell and Adams, 1982). It is a mixed cation current
76 mediated by HCN channels that are permeable to both K^+ and Na^+ ions under physiological conditions
77 (Biel et al., 2009; Wahl-Schott and Biel, 2009). HCN channels exert a crucial role in membrane
78 excitability (see Kase and Imoto, 2012 for review) and are involved in the main control of resting
79 membrane potential (RMP) (Pape et al., 1996; Doan et al., 1999; Lupica et al., 2001; Nolan et al.,
80 2007). Furthermore, I_h may modulate several other neuronal processes, such as dendritic integration
81 (Magee, 1998; 1999; 2000) and synaptic transmission (Beaumont and Zucker, 2000; Beaumont et al.,
82 2002). HCN activity may be regulated by cyclic nucleotides, such as cAMP (DiFrancesco and
83 Tortora, 1991) and GIRK channels (Kim and Johnston, 2015).
84 Consistent with its rewarding property, EtOH enhances the amplitude of I_h in dopaminergic neurons
85 of the ventral tegmental area (VTA) with an associated increase in firing rate and neuronal excitation

(Brodie and Appel, 1998; Bassareo et al., 2019), an effect reversed by the selective blocker of HCN, ZD7288 (Okamoto et al., 2006). Furthermore, Yan et al. (2009) demonstrated that EtOH increases the firing rate also in hippocampal GABAergic interneurons, in a concentration-dependent manner, through the positive modulation of HCN function.

In addition, a preclinical study performed using the intermittent alcohol consumption paradigm during early adolescence shows a significant reduction of I_h and altered excitability in medial prefrontal cortex pyramidal neurons (Salling et al., 2018). Interestingly, the involvement of HCN channels in the upregulation of alcohol consumption has been demonstrated in HCN1 constitutive knockout mice (Salling and Harrison, 2020).

Conversely, gene knockdown of HCN2 ion channels in the VTA markedly reduces voluntary EtOH intake in alcohol-preferring rats, supporting the notion that these channels may be potential therapeutic targets for alcohol use disorders (Salinas-Luypaert et al., 2022).

Since the effect of EtOH on HCN was characterized mainly in hippocampal GABAergic interneurons but not on principal neurons, which also highly express HCN, the main goal of the present study was to outline the potential modulatory effects of pharmacologically active concentrations (10 - 80 mM) of EtOH on HCN-mediated I_h recorded in rat CA3 principal neurons. We also evaluated whether EtOH modulation of I_h could be relevant for membrane excitability and synaptic integration and attempted to identify a possible mechanism of action for this drug of abuse.

2. Methods

2.1. Animals

Male Sprague Dawley CD rats (30-40 days of age) (Charles River, Como, Italy) were bred in our animal facility and maintained under an artificial 12 h light, 12 h dark cycle (light on from 08:00 to 20:00 hours), at constant temperature of 22° ± 2°C, and a relative humidity of 65%. They always had free access to water and standard laboratory food.

Animal care and handling throughout the experimental procedures were following the guidelines for care and use of experimental animals of the European Community Council (2010/63/UE L 276 20/10/2010) and the Italian law (DL 04/03/2014, no. 26). The study was also approved by the Organization for Animal Care of the University of Cagliari (OPBA-UniCA). Every needed effort was made to minimize animal pain and discomfort and to reduce the number of experimental subjects.

2.2. Preparation of rat hippocampal slices

Animals were deeply anesthetized with 5% isoflurane and decapitated. Brains were rapidly removed from the skull and transferred into an ice-cold modified artificial cerebrospinal fluid (ACSF) containing (in mM): 220 sucrose, 3 KCl, 6 $MgSO_4$, 0.2 $CaCl_2$, 26 $NaHCO_3$, 1.25 NaH_2PO_4, 10 D-glucose; pH 7.4 equilibrated with bubbling of 95% O_2 and 5% CO_2. Coronal brain slices (thickness of 250 μm) were prepared using a Leica VT1200s vibratome (Leica Microsystems, Milan, Italy). Slices were then transferred immediately to a nylon net submerged in normal ACSF containing (in mM): 126 NaCl, 3 KCl, 1.25 NaH_2PO_4, 1 $MgSO_4$, 2 $CaCl_2$, 10 glucose, and 26 $NaHCO_3$, pH 7.4, continuously bubbled with 95% O_2 and 5% CO_2. Slices were first kept at 34°C for 40 min and then for at least 30 min at room temperature before beginning of the experiments. For all recordings, the temperature of the bath was maintained at 34 °C.

2.3. Whole-cell patch-clamp recordings

Each hemi-slice was transferred to the recording chamber, which was constantly perfused with ACSF at a flow rate of 2 ml/min. Neurons were visualized with an infrared-differential interference contrast microscope (Olympus). Recording pipettes were prepared from borosilicate glass (outer diameter, 1.5 mm; inside diameter 0.86 mm, Sutter instruments, Novato, CA, USA) using a Flaming/Brown micropipette puller (Model P-97, Molecular Devices, Novato, CA, USA). The resistance of the pipettes ranged from 2.5 to 4.5 MΩ when they were filled with an internal solution containing (in mM): 140 potassium gluconate, 4 KCl, 0.1 EGTA, 10 HEPES, 2 MgATP, pH adjusted to 7.3 with

KOH. To elicit the hyperpolarization-activated currents (I_h), voltage-clamp recordings were performed with incremental hyperpolarizing steps of 10 mV of the membrane from -65 to -115 mV. For experiments involving the full activation of HCN channels, the first step from -40 mV to -120 mV was given, and subsequently, the membrane voltage was stepped back to potentials ranging from -120 to -40 mV (with 10 mV intervals). Membrane currents were recorded with an Axopatch 200-B amplifier (Axon Instruments, Foster City, CA, USA), filtered at 2 kHz, and digitized at 5 kHz, and pClamp 10.2 software (Molecular Devices, Union City, CA, USA) was used for acquisition, which allowed us to measure various characteristics of the neuronal membrane. Only recordings with access resistance of < 25-30 MΩ were used for analysis. Series resistance was not compensated, and cells were excluded from further analysis if access resistance changed by >20% during the recording. Off-line analysis of I_h was performed with Clampfit 10.2 software (Molecular Devices, Union City, CA, USA). The amplitude of I_h was measured as the difference between the maximum sag reached by membrane current during every voltage step compared with the steady-state level at the end of every step. In a different set of experiments, to evaluate synaptic integration, a bipolar concentric stimulation electrode (FHC, Bowdoin, ME, USA) was placed on the stratum radiatum of hippocampal CA3 subregion, and whole-cell recordings were performed in response to a train of four stimuli at 20 Hz. Membrane potential was maintained at a value ranging from -75 to -90 mV to prevent action potentials. These experiments were performed in the presence of low [Ca^{2+}] to suppress facilitation from repeated stimulation, 3 mM $MgSO_4$ to block NMDA receptors, 20 μM bicuculline and 10 μM SCH50911 to block GABAergic transmission.

2.4. Statistics

Statistical analysis was performed using Graph Pad Prism 7 (GraphPad Software, San Diego, CA). Results were analyzed using columns statistics test and one-way analysis of variance (ANOVA) with Bonferroni post hoc test. A P value < 0.05 was considered statistically significant. Data are expressed as means ± SEM.

164

165 *2.5. Drugs*

166 All drugs were bath-applied unless otherwise indicated and were purchased from Sigma (Sigma-
167 Aldrich, Milan, Italy). Most of them were hydrochloride salts and were dissolved in ACSF to make
168 stock solutions. Bicuculline was dissolved in dimethylsulfoxide (DMSO) >99.9%, as stock solution,
169 and after dilution, the DMSO concentration was less than 0.1%.

170

171 **3. Results**

172

173 *3.1. Characterization of I_h in rat CA3 pyramidal neurons*

174 We began our study by characterizing some of the neurophysiological properties of I_h in rat CA3
175 pyramidal neurons. Under voltage-clamp conditions, the application of voltage steps (each of 2 s
176 duration) from -40 to -120 mV (with 10 mV increments) elicited a slowly activating inward current
177 whose amplitude increased as the membrane voltage was progressively raised to -120 mV (Fig. 1A).
178 Averaged steady-state I_h amplitude measured by hyperpolarizing the cell membrane at -120 mV was
179 -158.3 ± 8.96 pA (n = 87) which, after normalizing to the membrane capacitance, resulted in a value
180 of -0.79 ± 0.04 pA/pF (n = 87). I-V curve revealed that activation of I_h occurred at an apparent
181 membrane potential higher than -70 mV, with a linear relationship between -70 to -120 mV having a
182 calculated slope value of 60 ± 1.3 pS/pF (n = 4) (Fig. 1B). By applying the protocol proposed by
183 Maccaferri and McBain (1996), the fully activated I_h I-V relationship and the I_h reversal potential
184 were established and calculated as depicted in Fig. 1C and D. In detail, following a voltage step from
185 -40 to -120 mV (2 s duration), the membrane voltage was stepped to potentials ranging from -120 to
186 -40 mV (with 10 mV intervals). The resulting I-V relationship was linear and had a slope value of
187 107 ± 4.7 pS/pF (n = 4). The extrapolated reversal potential was -31 ± 0.8 mV (n = 4) (Fig. 1D). The
188 raise phase of I_h could be fitted by a two-component exponential equation, with a fast component of
189 82 ± 11 ms (n = 10) and a slow component of 393 ± 56 ms (n = 10). In agreement with previous

reports (Maccaferri and McBain, 1996; Biel et al., 2009), I_h-mediated sags were suppressed by applying either the non-selective channel blocker CsCl (5 mM) or the selective blocker ZD7288 (20 μM) (Fig. 1E).

3.2. Ethanol bi-directionally modulates HCN-mediated I_h in CA3 pyramidal neurons

To investigate whether HCN-mediated I_h recorded in CA3 pyramidal neurons might be modulated acutely by the bath-perfusion of slices with EtOH, we initially tested a wide range (10 – 80 mM) of concentrations, as illustrated in Fig. 2A. Each concentration of EtOH was bath-applied for 10-15 minutes during continuous voltage-clamp recordings, and I_h was evoked every 20 s by hyperpolarizing the cell membrane from the holding potential (-65 mV) to -115 mV. A bi-directional and significant concentration-dependent effect of EtOH was found [$F_{(8,209)} = 8.332$; $P < 0.0001$]. Perfusion of 20 mM EtOH resulted in a significant increase in the amplitude of I_h (34.2 ± 5.9%, n = 22, $P < 0.001$) with respect to the baseline response (Fig. 2A-C). Conversely, 80 mM EtOH produced an opposite effect, with a significant reduction (53.1 ± 9.5%; n = 13, $P < 0.001$) of I_h amplitude (Fig 2A-C). All these effects appeared evident after about 10-15 minutes of continuous bath perfusion of EtOH and were relatively slowly reversible after at least 10 min of drug washout (Fig. 2D). Based on the concentration-response curve, all the subsequent experiments were conducted by testing only the concentrations of 20 and 80 mM EtOH as the most representative for the dual modulatory effect of this drug on I_h.

Analysis of the effects of EtOH on the kinetics of I_h showed that 20 mM EtOH slightly accelerated, whereas 80 mM significantly slowed down, the fast component of the I_h raising phase (Fig. 2E). Furthermore, neither of the two concentrations of EtOH altered the membrane potential at which I_h was activated when membrane potential was stepped progressively from -40 to -120 mV (Fig. 2F). In the fully activated I-V curve, where membrane potential was first hyperpolarized to -120 mV (for 2 s), and then brought to potentials from -120 to -40 mV (with 10 mV intervals), bath perfusion of 20 and 80 mM EtOH altered again in an opposite manner the slope of the I-V relationship but did not

modify the I_h reversal potential (Control, -30 mV; 20 mM EtOH, -28 mV; 80 mM EtOH, -34 mV) (Fig. 2G).

In the attempt to determine whether EtOH might directly interact with HCN to bi-directionally modulate I_h, we tested the two concentrations (20 and 80 mM) of EtOH in the presence of a relatively low concentration (1 μM) of the selective HCN blocker ZD7288. At this concentration, ZD7288 reduced baseline I_h amplitude by 65 ± 9.7% (n = 6) (Fig. 2H). After a pre-incubation of 5 min with ZD7288, to reach its steady state effect on HCN cannels, both low and high concentration of EtOH failed to significantly alter the amplitude of I_h suggesting that ZD7288 may interfere with EtOH for a direct interaction with the channel (Fig. 2H).

3.3. Effect of EtOH on postsynaptic integration in CA3 pyramidal neurons

Previous studies have well documented that HCN channels play an important role in controlling the temporal summation of post-synaptic potentials (PSPs) in different brain regions contributing actively to the integration of neuronal excitatory signals (Magee, 1999; Sheets et al., 2011; Masi et al., 2013). To elucidate the effects of EtOH on PSP summation and synaptic integration, we delivered a train of 4 electrical stimuli of the same intensity and with a frequency of 20 Hz, to distal dendrites of CA3 pyramidal neurons. For isolating EPSPs that were mediated specifically by the AMPA/kainate subtype of glutamate receptors, the extracellular ACSF solution was modified as to contain an increased concentration of Mg^{2+} (3 mM) to block NMDA receptors, bicuculline (20 μM), and SCH-50911 (10 μM), antagonists of the $GABA_A$ and $GABA_B$ receptor, respectively. In addition, the Ca^{2+} concentration in the ACSF was lowered to 0.5 mM to prevent the event of post-synaptic facilitation inducible by repeated stimulations. Like results obtained previously in other brain regions (Masi et al., 2013), this protocol produced in CA3 pyramidal neurons a marked temporal summation of the responses, as measured by the ratio of the amplitude of the fourth related to the first EPSP (Fig. 3A). Bath application of the selective HCN blocker ZD7288 (20 μM) induced a significant ($P < 0.05$; n = 3) increase in temporal summation compared to baseline (Fig. 3A and B). Perfusion of EtOH (20

mM) led to a significant ($P < 0.05$; n = 9) decrease of the temporal EPSP summation compared to baseline (Fig. 3C, D) whereas bath application of 80 mM EtOH, similarly to the effect of ZD7288, significantly ($P < 0.001$; n = 6) increased the temporal summation ratio (Fig. 3E, F).

3.4. Effect of EtOH on neuronal firing in CA3 pyramidal neurons

HCN channel activity plays an essential control in neuronal action potential firing rate, as shown previously in both midbrain dopamine and hippocampal CA3 interneurons (Cobb et al., 2003; Okamoto et al., 2006). We thus investigated whether EtOH might be capable of altering neuronal firing in CA3 pyramidal neurons through a mechanism involving the HCN channels. In our experimental conditions, when we bath-perfused hippocampal slices with normal ACSF, CA3 pyramidal neurons displayed virtually no spontaneous firing activity (Jochems and Yoshida, 2013). This was expected since in acute slices, a significant portion of the original neuronal dendritic network is lost, allowing the relatively intact GABAergic axons to exert a dominant inhibitory tone against glutamatergic excitation (Okamoto et al., 2014), with the result that the level of spontaneous activity can be dramatically reduced. Consequently, action potential firing was evoked by perfusing hippocampal slices with ACSF containing 10 mM KCl, together with bicuculline (20 µM) and kynurenic acid (1 mM) to block inhibitory GABA-A and excitatory glutamate receptors, respectively. The resulting firing activity (3.1 ± 0.8 Hz, n = 6) was almost completely suppressed (-85.4 ± 3.4%, n = 3) by 20 µM ZD 7288 (Fig. 4A and B) and again bi-directionally modulated by 20 (58.3 ± 16.1%, n = 5) and 80 mM (-44.6 ± 13.2%, n = 5) EtOH as illustrated in Fig. 4A and C.

3.5. Modulation of I_h by the dopamine/cAMP/PKA intracellular pathway

The function of HCN is physiologically modulated by different intracellular cyclic nucleotides, including cAMP (DiFrancesco and Tortora, 1991; Chen et al., 2001; Santoro et al., 1998). It has been reported that, in the entorhinal cortex, dopamine D1 receptor-mediated elevation of cAMP and activation of the cAMP-dependent protein kinase A (PKA) can modulate neuronal excitability

through the interaction with HCN channels (Rosenkranz and Johnston, 2006). Consequently, we conducted a series of experiments on establishing whether the modulatory action of EtOH on I_h recorded in CA3 pyramidal neurons might interact with or involve the cAMP/PKA intracellular pathway.

To test whether, in our experimental conditions, the cAMP/PKA pathway may regulate HCN-mediated I_h currents, dopamine (10 μM) was bath-applied acutely for 5 min to hippocampal slices, and I_h amplitude (evoked by a step of membrane potential to -115 mV) was continuously monitored. The I_h amplitude increased upon the termination of dopamine perfusion with a significant effect (47 ± 9.5% *vs*. baseline; $P < 0.05$, n = 10) that was apparent 15 min after dopamine perfusion and that further increased during the 40 min of recording, reaching a maximal value around 70% (Fig. 5A, B). The enhancing effect of dopamine of I_h amplitude was prevented by the pre-application for 15 min of either the D1 receptor antagonist SCH23390 (5 μM), or the selective adenylyl cyclase inhibitor 2',3'-dideoxyadenosine (DDA) (Kim et al., 1994; Ribas Pereira et al., 2015) at the concentration of 10 μM. The latter compound also induced per se a modest, not statistically significant, reduction of I_h amplitude, suggesting a relatively low adenylyl cyclase basal activity (Fig. 5A, B).

The activity of adenylyl cyclase can be directly stimulated with forskolin (Alasbahi and Melzig, 2012), and this effect results in an enhancement of HCN activity (Dibattista et al., 2008). Forskolin was then tested in CA3 pyramidal neurons at different concentrations, ranging from 0.1 to 30 μM. As shown in Fig. 6, bath-application of 0.1 μM forskolin increased by 36 ± 11.2 % ($P < 0.05$, n = 5) the amplitude of I_h above baseline value. On the contrary, at the concentration of 30 μM, forskolin had an opposite effect, reducing the same parameter by 28 ± 7.4% ($P < 0.05$, n = 4) (Fig. 6A). The bidirectional effect of forskolin was abolished in the presence of the selective inhibitor of PKA, H89 (Marunaka et al., 2003). Interestingly, pre-application for 15 min of 10 μM H89, which did not affect the amplitude of I_h by itself was able to block the modulatory action of low concentration (0.1 μM) of forskolin but failed to modify that produced by higher (30 μM) concentrations (Fig. 6C).

We then tested whether the modulatory actions of EtOH on I_h would be modified during the co-application of DDA or H89. As shown in the Fig 7, the effect of 20 mM EtOH (29 ± 7.8% *vs*. baseline, n = 4, $P < 0.05$), and 80 mM EtOH (-44 ± 11.8 *vs*. baseline, n = 6, $P < 0.001$) were completely occluded by both DDA and H89.

4. Discussion

Previous studies have suggested that HCN channels expressed in mouse midbrain dopamine neurons (Brodie and Appel, 1998) and rat hippocampal interneurons (Yan et al., 2009) are potential molecular targets for the EtOH actions at pharmacological concentrations (Okamoto et al., 2006; Yan et al., 2009). In the present study, we have assessed the acute effects of EtOH on HCN-mediated I_h in rat CA3 pyramidal neurons, which have been shown to express HCN (Zhang et al., 2016), and attempted to pinpoint the possible molecular mechanisms underlying such action.

Our results show that at the relatively lower concentration of 20 mM, EtOH significantly increases I_h amplitude, whereas concentrations above 60 mM modulate the I_h sag negatively, suggesting a potential biphasic modulatory activity of this drug on the function of HCN channels. The positive modulation induced by the 20 mM EtOH observed in our study agrees with other reports performed in hippocampal and VTA neurons (Okamoto et al. 2006; Yan et al., 2009). While we are not in line comparing the effects of higher EtOH, which in those same reports was shown that 100 mM EtOH increased I_h amplitude in both midbrain dopaminergic neurons and hippocampal GABAergic interneurons (Okamoto et al., 2006; Yan et al., 2009). These observations suggest the hypothesis that the effects of EtOH on HCN function might be dependent on the brain area as well as the neuronal subpopulation studied and be also related, at least in part, to the differential expression of HCN isoforms in different neuronal types, such as those reported in the hippocampal formation (Robinson and Siegelbaum, 2003). In particular, the HCN1 subunit is mainly expressed in CA1 pyramidal neurons, while CA3 pyramidal neurons show a higher expression of the HCN2 isoform, differently

by GABAergic interneurons that indistinctly express both isoforms (Robinson and Siegelbaum, 2003).

HCN channels are strongly involved in the control of synaptic integration and EPSP summation of both inhibitory and excitatory signals (Magee, 1999). EPSP summation is a process that is regulated by the remarkable distribution of HCN channels along the neuronal dendritic arborization. This critical role of HCN has been demonstrated in several neuronal subpopulations, such as the hippocampal pyramidal CA1 pyramidal cells (Magee, 1999). It also has been reported that a decrease in HCN expression and function leads to an enhancement of EPSP summation (Magee, 1999). In our data collected in CA3 pyramidal neurons, the summation of 4 electrically evoked AMPAR-mediated EPSPs was markedly enhanced in the presence of the HCN selective blocker ZD7288, an effect that is mimicked by the perfusion of higher concentrations of EtOH, suggesting a common antagonistic action of both drugs on HCN channels. Interestingly, consistent with the increase in I_h amplitude, 20 mM EtOH produced a parallel decrease in EPSP summation. Furthermore, because our recordings were performed in the presence of antagonists of GABAA and GABAB receptors, as well as in the presence of high Mg^{2+} concentrations to block NMDA-receptors, we can exclude that these modulatory effects are dependent on the interaction between EtOH and inhibitory or additional glutamatergic excitatory inputs. This finding supports the idea that pharmacological or molecular ablation of HCN-mediated I_h may lead to a facilitation of dendritic temporal summation (Kim et al., 2012). In line with our findings, Masi and coworkers demonstrated that 1-methyl-4-phenylpyridinium (MPP+), which markedly reduces HCN function, enhances the summation of EPSP in dopamine neurons onto substantia nigra pars compacta (Masi et al., 2013).

Since the activity of HCN is regarded as a contributing factor in the fine-tuning of neuronal excitability (Magee, 1998;1999; Chen et al., 2001; Beck and Yaari, 2008; Brager and Johnston, 2007), we tested whether the effect of EtOH on action potential firing in hippocampal CA3 pyramidal neurons might involve its interaction with HCN channels. The idea that HCN channels exert a fine-tuning of neuronal firing rate was here further confirmed, as the perfusion of the selective HCN

blocker, ZD-7288 (20 μM), almost completely inhibited the K^+-induced action potential firing activity recorded in CA3 neurons. The use of ACSF containing high K^+ (10 mM) was crucial because in our experimental condition, and in line with other reports (Jochems and Yoshida, 2013), CA3 pyramidal cells do not present a spontaneous and persistent firing activity in slice recordings. In such conditions, EtOH (20 mM) increased the K^+-induced firing frequency, while higher concentrations (80 mM) reduced this parameter. The modulatory activity of EtOH on neuronal firing is well established by previous experimental evidence. More precisely, EtOH reduces the firing rate of pyramidal neurons with regular activity in the somatosensory cortex (Sessler et al., 1998) and inhibits neuronal activity in pyramidal cells of the prefrontal cortex (Tu et al., 2007). Other evidence demonstrated that acute EtOH perfusion enhanced neuronal firing in dopaminergic cells in VTA (Brodie and Appel, 1998; Appel et al., 2003; Okamoto et al., 2006; Bassareo et al., 2019), in which HCN channels are strongly expressed and can regulate the firing properties of these neurons. Because EtOH can modulate the firing rate of principal neurons also by interacting with the GABAergic system (Wakita et al., 2012), in our experimental conditions we excluded this effect using the GABAA receptor antagonist bicuculline, together with the ionotropic glutamate receptor antagonist kynurenic acid, to isolate the potential effect of EtOH onto HCN channels.

Intracellular messengers, such as cyclic nucleotides and protein kinases, are recognized as potent modulators of HCN function, and PKA-dependent phosphorylation sites are present in HCN channel structure (Santoro et al., 1998). In agreement with these findings, bath perfusion of dopamine increased the amplitude of I_h also in CA3 pyramidal neurons, and this effect was blocked by the selective D1R antagonist SCH23390, suggesting that the dopamine-induced modulation of HCN occurs through the activation of D1Rs. Our data are in accordance with previous reports demonstrating that dopamine positively enhances I_h amplitude in mPFC pyramidal neurons through D1R stimulation (Gamo et al., 2015). In agreement, the dopamine effect on I_h amplitude is prevented by bath application of adenylyl cyclase inhibitor DDA. Interestingly, DDA failed to induce any significant effect when perfused alone, suggesting that the basal activity of adenylyl cyclase maintains

intracellular levels of cAMP that may not be sufficient for tonic activation of HCN function. Furthermore, as expected, the adenyl cyclase stimulator forskolin mimics the effect showed by dopamine when low concentration (0.1 μM) was tested. However, as similarly observed with EtOH, when a higher concentration (up to 30 μM) of forskolin was applied to the slice, an opposite inhibitory action on I_h was detected. The pharmacological profile showed by EtOH was thus like that observed for forskolin. In addition, perfusion of the selective inhibitor of cAMP-dependent protein kinases A (PKA), H89, completely suppressed the modulatory activity on HCN channels evoked by forskolin suggesting that the inhibition of forskolin-triggered intracellular cascade may prevent its action on HCN. Furthermore, we also found that DDA and H89 could antagonize the modulatory effects of EtOH at lower and higher concentrations in a similar way as forskolin, suggesting that the cAMP/AC/PKA intracellular pathway may represent a potential target for EtOH-induced modulation of HCN channels. It is well known that adenylyl cyclase is a relevant molecular target of EtOH actions (Tabakoff et al., 2001; Kou and Yoshimura, 2007). In line with our data, EtOH showed two opposing effects on the activity of adenylyl cyclase, exerting an enhancement at lower concentrations and an inhibition at higher (Gupta et al., 2013). This evidence strongly supports our results where low EtOH concentrations enhance HCN-mediated I_h currents, whereas high concentrations inhibit them with a mechanism that involves AC. These data prompted us to speculate that the absolute intracellular levels of cAMP may be crucial in the modulatory action of HCN function, where lower concentrations facilitate HCN activity and higher exert opposite effects.

5. Conclusions

Overall, our findings demonstrate that EtOH may exert its modulatory effect on CA3 pyramidal neurons by interacting with HCN channels and, in turn, with the downstream intracellular pathways, an effect that is dependent on the concentration. This dual pharmacological profile showed by EtOH (low vs high concentrations) appears to be relevant in many neurophysiological aspects that involve the activity of HCN channels, such as neuronal firing and temporal summation of postsynaptic

potentials. Finally, although our results lack to demonstrate a direct interaction of EtOH with HCN channels, EtOH may regulate HCN function indirectly through a molecular mechanism that appears to involve its interaction with the AC/cAMP/PKA intracellular pathway.

Acknowledgments

The authors wish to thank Prof. Laura Dazzi for her invaluable insights on the manuscript, and Mr. Giancarlo Porcu and Mr. Marco Sechi for their technical assistance in maintaining the animal colony.

CRediT autorship contribution statement

Valentina Licheri: Investigation - wiriting – original draft. **Giuseppe Talani**: data curation - methodology. **Giovanni Biggio**: supervision. **Enrico Sanna**: conceptualization – writing & editing

Declaration of competing interest

The authors have no competing interests to declare that are relevant to the content of this article.

Data availability

Data will be made available on request**.**

Funding

The work presented was supported by Faculty Research Founding to G.B. and E.S.

References

Abrahao KP, Salinas AG, Lovinger DM. Alcohol and the Brain: Neuronal Molecular Targets, Synapses, and Circuits. Neuron. 2017 Dec 20;96(6):1223-1238. doi: 10.1016/j.neuron.2017.10.032. Review. PubMed PMID: 29268093; PubMed Central PMCID: PMC6566861.

Alasbahi RH, Melzig MF. Forskolin and derivatives as tools for studying the role of cAMP. Pharmazie. 2012 Jan;67(1):5-13. Review. PubMed PMID: 22393824.

Appel SB, Liu Z, McElvain MA, Brodie MS. Ethanol excitation of dopaminergic ventral tegmental area neurons is blocked by quinidine. J Pharmacol Exp Ther. 2003 Aug;306(2):437-46. doi: 10.1124/jpet.103.050963. Epub 2003 Apr 29. PubMed PMID: 12721326.

Bader CR, Macleish PR, Schwartz EA. A voltage-clamp study of the light response in solitary rods of the tiger salamander. J Physiol. 1979 Nov;296:1-26. doi: 10.1113/jphysiol.1979.sp012988. PubMed PMID: 529060; PubMed Central PMCID: PMC1279061.

Bassareo V, Talani G, Frau R, Porru S, Rosas M, Kasture SB, Peana AT, Loi E, Sanna E, Acquas E. Inhibition of Morphine- and Ethanol-Mediated Stimulation of Mesolimbic Dopamine Neurons by Withania somnifera. Front Neurosci. 2019;13:545. doi: 10.3389/fnins.2019.00545. eCollection 2019. PubMed PMID: 31275092; PubMed Central PMCID: PMC6593272.

Beaumont V, Zhong N, Froemke RC, Ball RW, Zucker RS. Temporal synaptic tagging by I(h) activation and actin: involvement in long-term facilitation and cAMP-induced synaptic enhancement. Neuron. 2002 Feb 14;33(4):601-13. doi: 10.1016/s0896-6273(02)00581-0. PubMed PMID: 11856533.

Beaumont V, Zucker RS. Enhancement of synaptic transmission by cyclic AMP modulation of presynaptic Ih channels. Nat Neurosci. 2000 Feb;3(2):133-41. doi: 10.1038/72072. PubMed PMID: 10649568.

Beck H, Yaari Y. Plasticity of intrinsic neuronal properties in CNS disorders. Nat Rev Neurosci. 2008 May;9(5):357-69. doi: 10.1038/nrn2371. Review. PubMed PMID: 18425090.

Biel M, Wahl-Schott C, Michalakis S, Zong X. Hyperpolarization-activated cation channels: from genes to function. Physiol Rev. 2009 Jul;89(3):847-85. doi: 10.1152/physrev.00029.2008. Review. PubMed PMID: 19584315.

Brager DH, Johnston D. Plasticity of intrinsic excitability during long-term depression is mediated through mGluR-dependent changes in I(h) in hippocampal CA1 pyramidal neurons. J Neurosci. 2007 Dec 19;27(51):13926-37. doi: 10.1523/JNEUROSCI.3520-07.2007. PubMed PMID: 18094230; PubMed Central PMCID: PMC6673524.

Brodie MS, Appel SB. The effects of ethanol on dopaminergic neurons of the ventral tegmental area studied with intracellular recording in brain slices. Alcohol Clin Exp Res. 1998 Feb;22(1):236-44. PubMed PMID: 9514313.

Chen S, Wang J, Siegelbaum SA. Properties of hyperpolarization-activated pacemaker current defined by coassembly of HCN1 and HCN2 subunits and basal modulation by cyclic nucleotide. J Gen Physiol. 2001 May;117(5):491-504. doi: 10.1085/jgp.117.5.491. PubMed PMID: 11331358; PubMed Central PMCID: PMC2233656.

Chen Y, Wu P, Fan X, Chen H, Yang J, Song T, Huang C. Ethanol enhances human hyperpolarization-activated cyclic nucleotide-gated currents. Alcohol Clin Exp Res. 2012 Dec;36(12):2036-46. doi: 10.1111/j.1530-0277.2012.01826.x. Epub 2012 May 16. PubMed PMID: 22591131.

Cobb SR, Larkman PM, Bulters DO, Oliver L, Gill CH, Davies CH. Activation of Ih is necessary for patterning of mGluR and mAChR induced network activity in the hippocampal CA3 region. Neuropharmacology. 2003; 44(3):293-303. doi: 10.1016/S0028-3908(02)00405-7.

Diamond I, Messing RO. Neurologic effects of alcoholism. West J Med. 1994 Sep;161(3):279-87. Review. PubMed PMID: 7975567; PubMed Central PMCID: PMC1011410.

DiFrancesco D, Tortora P. Direct activation of cardiac pacemaker channels by intracellular cyclic AMP. Nature. 1991 May 9;351(6322):145-7. doi: 10.1038/351145a0. PubMed PMID: 1709448.

Dibattista M, Mazzatenta A, Grassi F, Tirindelli R, Menini A. Hyperpolarization-activated cyclic nucleotide-gated channels in mouse vomeronasal sensory neurons. J Neurophysiol. 2008 Aug;100(2):576-86. doi: 10.1152/jn.90263.2008. Epub 2008 May 28. PubMed PMID: 18509074.

Doan TN, Kunze DL. Contribution of the hyperpolarization-activated current to the resting membrane potential of rat nodose sensory neurons. J Physiol. 1999 Jan 1;514 (Pt 1):125-38. doi: 10.1111/j.1469-7793.1999.125af.x. PubMed PMID: 9831721; PubMed Central PMCID: PMC2269051.

Egervari G, Siciliano CA, Whiteley EL, Ron D. Alcohol and the brain: from genes to circuits. Trends Neurosci. 2021 Dec;44(12):1004-1015. doi: 10.1016/j.tins.2021.09.006. Epub 2021 Oct 23. Review. PubMed PMID: 34702580; PubMed Central PMCID: PMC8616825.

Gamo NJ, Lur G, Higley MJ, Wang M, Paspalas CD, Vijayraghavan S, Yang Y, Ramos BP, Peng K, Kata A, Boven L, Lin F, Roman L, Lee D, Arnsten AF. Stress Impairs Prefrontal Cortical Function via D1 Dopamine Receptor Interactions With Hyperpolarization-Activated Cyclic Nucleotide-Gated Channels. Biol Psychiatry. 2015 Dec 15;78(12):860-70. doi: 10.1016/j.biopsych.2015.01.009. Epub 2015 Feb 4. PubMed PMID: 25731884; PubMed Central PMCID: PMC4524795.

Gupta R, Qualls-Creekmore E, Yoshimura M. Real-time monitoring of intracellular cAMP during acute ethanol exposure. Alcohol Clin Exp Res. 2013 Sep;37(9):1456-65. doi: 10.1111/acer.12133. Epub 2013 Jun 3. PubMed PMID: 23731206; PubMed Central PMCID: PMC3776015.

Halliwell JV, Adams PR. Voltage-clamp analysis of muscarinic excitation in hippocampal neurons. Brain Res. 1982 Oct 28;250(1):71-92. doi: 10.1016/0006-8993(82)90954-4. PubMed PMID: 6128061.

Harris RA, Trudell JR, Mihic SJ. Ethanol's molecular targets. Sci Signal. 2008 Jul 15;1(28):re7. doi: 10.1126/scisignal.128re7. Review. PubMed PMID: 18632551; PubMed Central PMCID: PMC2671803.

Jochems A, Yoshida M. Persistent firing supported by an intrinsic cellular mechanism in hippocampal CA3 pyramidal cells. Eur J Neurosci. 2013 Jul;38(2):2250-9. doi: 10.1111/ejn.12236. Epub 2013 May 8. PubMed PMID: 23651161.

Jung YC, Namkoong K. Alcohol: intoxication and poisoning - diagnosis and treatment. Handb Clin Neurol. 2014;125:115-21. doi: 10.1016/B978-0-444-62619-6.00007-0. Review. PubMed PMID: 25307571.

Kase D, Imoto K. The Role of HCN Channels on Membrane Excitability in the Nervous System. J Signal Transduct. 2012;2012:619747. doi: 10.1155/2012/619747. Epub 2012 Aug 13. PubMed PMID: 22934165; PubMed Central PMCID: PMC3425855.

Kim CS, Chang PY, Johnston D. Enhancement of dorsal hippocampal activity by knockdown of HCN1 channels leads to anxiolytic- and antidepressant-like behaviors. Neuron. 2012 Aug 9;75(3):503-16. doi: 10.1016/j.neuron.2012.05.027. PubMed PMID: 22884333; PubMed Central PMCID: PMC3418514.

Kim C, Park D, Ryu K. Effect of adenylate cyclase inhibitor and protein kinase C inhibitor on GnRH-induced LH release and LH beta subunit biosynthesis in rat anterior pituitary cells. Yonsei Med J. 1994 Dec;35(4):493-501. doi: 10.3349/ymj.1994.35.4.493. PubMed PMID: 7871854.

Kim CS, Johnston D. A1 adenosine receptor-mediated GIRK channels contribute to the resting conductance of CA1 neurons in the dorsal hippocampus. J Neurophysiol. 2015 Apr 1;113(7):2511-23. doi: 10.1152/jn.00951.2014. Epub 2015 Feb 4. PubMed PMID: 25652929; PubMed Central PMCID: PMC4416607.

Kou J, Yoshimura M. Isoform-specific enhancement of adenylyl cyclase activity by n-alkanols. Alcohol Clin Exp Res. 2007 Sep;31(9):1467-72. doi: 10.1111/j.1530-0277.2007.00455.x. PubMed PMID: 17760784.

549 Lupica CR, Bell JA, Hoffman AF, Watson PL. Contribution of the hyperpolarization-activated
550 current (I(h)) to membrane potential and GABA release in hippocampal interneurons. J
551 Neurophysiol. 2001 Jul;86(1):261-8. doi: 10.1152/jn.2001.86.1.261. PubMed PMID: 11431507.
552
553 Maccaferri G, McBain CJ. The hyperpolarization-activated current (Ih) and its contribution to
554 pacemaker activity in rat CA1 hippocampal stratum oriens-alveus interneurones. J Physiol. 1996
555 Nov 15;497 (Pt 1):119-30. doi: 10.1113/jphysiol.1996.sp021754. PubMed PMID: 8951716;
556 PubMed Central PMCID: PMC1160917.
557
558 Magee JC. Dendritic hyperpolarization-activated currents modify the integrative properties of
559 hippocampal CA1 pyramidal neurons. J Neurosci. 1998 Oct 1;18(19):7613-24. PubMed PMID:
560 9742133; PubMed Central PMCID: PMC6793032.
561
562 Magee JC. Dendritic integration of excitatory synaptic input. Nat Rev Neurosci. 2000
563 Dec;1(3):181-90. doi: 10.1038/35044552. Review. PubMed PMID: 11257906.
564
565 Magee JC. Dendritic lh normalizes temporal summation in hippocampal CA1 neurons. Nat
566 Neurosci. 1999 Jun;2(6):508-14. doi: 10.1038/9158. PubMed PMID: 10448214.
567
568 Marunaka Y, Niisato N. H89, an inhibitor of protein kinase A (PKA), stimulates Na+ transport by
569 translocating an epithelial Na+ channel (ENaC) in fetal rat alveolar type II epithelium. Biochem
570 Pharmacol. 2003 Sep 15;66(6):1083-9. doi: 10.1016/s0006-2952(03)00456-8. PubMed PMID:
571 12963496.
572
573 Masi A, Narducci R, Landucci E, Moroni F, Mannaioni G. MPP(+) -dependent inhibition of Ih
574 reduces spontaneous activity and enhances EPSP summation in nigral dopamine neurons. Br J
575 Pharmacol. 2013 May;169(1):130-42. doi: 10.1111/bph.12104. PubMed PMID: 23323755; PubMed
576 Central PMCID: PMC3632244.
577
578 Nolan MF, Dudman JT, Dodson PD, Santoro B. HCN1 channels control resting and active
579 integrative properties of stellate cells from layer II of the entorhinal cortex. J Neurosci. 2007 Nov
580 14;27(46):12440-51. doi: 10.1523/JNEUROSCI.2358-07.2007. PubMed PMID: 18003822;
581 PubMed Central PMCID: PMC6673323.
582

Noma A, Irisawa H. Membrane currents in the rabbit sinoatrial node cell as studied by the double microelectrode method. Pflugers Arch. 1976 Jun 29;364(1):45-52. doi: 10.1007/BF01062910. PubMed PMID: 986617.

Okamoto K, Ishikawa T, Abe R, Ishikawa D, Kobayashi C, Mizunuma M, Norimoto H, Matsuki N, Ikegaya Y. Ex vivo cultured neuronal networks emit in vivo-like spontaneous activity. J Physiol Sci. 2014 Nov;64(6):421-31. doi: 10.1007/s12576-014-0337-4. Epub 2014 Sep 11. PubMed PMID: 25208897.

Okamoto T, Harnett MT, Morikawa H. Hyperpolarization-activated cation current (Ih) is an ethanol target in midbrain dopamine neurons of mice. J Neurophysiol. 2006 Feb;95(2):619-26. doi: 10.1152/jn.00682.2005. Epub 2005 Sep 7. PubMed PMID: 16148268; PubMed Central PMCID: PMC1454360.

Pape HC. Queer current and pacemaker: the hyperpolarization-activated cation current in neurons. Annu Rev Physiol. 1996;58:299-327. doi: 10.1146/annurev.ph.58.030196.001503. Review. PubMed PMID: 8815797.

Pereira GR, Lorenzo PL, Carneiro GF, Bilodeau-Goeseels S, Kastelic J, Liu IK. A specific adenylyl cyclase inhibitor (DDA) and a cyclic AMP-dependent protein kinase inhibitor (H-89) block the action of equine growth hormone on in vitro maturation of equine oocytes. Zygote. 2015 Dec;23(6):795-801. doi: 10.1017/S0967199414000434. Epub 2014 Sep 26. PubMed PMID: 25257826.

Robinson RB, Siegelbaum SA. Hyperpolarization-activated cation currents: from molecules to physiological function. Annu Rev Physiol. 2003;65:453-80. doi: 10.1146/annurev.physiol.65.092101.142734. Epub 2002 Nov 19. Review. PubMed PMID: 12471170.

Rosenkranz JA, Johnston D. Dopaminergic regulation of neuronal excitability through modulation of Ih in layer V entorhinal cortex. J Neurosci. 2006 Mar 22;26(12):3229-44. doi: 10.1523/JNEUROSCI.4333-05.2006. PubMed PMID: 16554474; PubMed Central PMCID: PMC6674109.

Salinas-Luypaert C, Sáez-Cortez F, Quintanilla ME, Herrera-Marschitz M, Rivera-Meza M. Gene knockdown of HCN2 ion channels in the ventral tegmental area reduces ethanol consumption in alcohol preferring rats. Am J Drug Alcohol Abuse. 2022 Mar 4;48(2):165-175. doi: 10.1080/00952990.2022.2033759. Epub 2022 Apr 4. PubMed PMID: 35377277.

Salling MC, Skelly MJ, Avegno E, Regan S, Zeric T, Nichols E, Harrison NL. Alcohol consumption during adolescence in a mouse model of binge drinking alters the intrinsic excitability and function of the prefrontal cortex through a reduction in the hyperpolarization-activated cation current. J Neurosci. 2018 Jul 4;38(27):6207-6222. doi: 101523/JNEUROSCI.0550-18.2018. . PubMed PMID: 29915134; PubMed Central PMCID: PMC6031577.

Salling MC, Harrison NL. Constitutive Genetic Deletion of Hcn1 increases alcohol preference during adolescence. Brain Sci. 2020 Oct 22; 10(11):763. doi: 10.3390/brainsci10110763. PubMed PMID: 33105624; PubMed Central PMCID: PMC7690419.

Santoro B, Liu DT, Yao H, Bartsch D, Kandel ER, Siegelbaum SA, Tibbs GR. Identification of a gene encoding a hyperpolarization-activated pacemaker channel of brain. Cell. 1998 May 29;93(5):717-29. doi: 10.1016/s0092-8674(00)81434-8. PubMed PMID: 9630217.

Santoro B, Tibbs GR. The HCN gene family: molecular basis of the hyperpolarization-activated pacemaker channels. Ann N Y Acad Sci. 1999 Apr 30;868:741-64. doi: 10.1111/j.1749-6632.1999.tb11353.x. Review. PubMed PMID: 10414361.

Sessler FM, Hsu FC, Felder TN, Zhai J, Lin RC, Wieland SJ, Kosobud AE. Effects of ethanol on rat somatosensory cortical neurons. Brain Res. 1998 Sep 7;804(2):266-74. doi: 10.1016/s0006-8993(98)00680-5. PubMed PMID: 9757061.

Sheets PL, Suter BA, Kiritani T, Chan CS, Surmeier DJ, Shepherd GM. Corticospinal-specific HCN expression in mouse motor cortex: I(h)-dependent synaptic integration as a candidate microcircuit mechanism involved in motor control. J Neurophysiol. 2011 Nov;106(5):2216-31. doi: 10.1152/jn.00232.2011. Epub 2011 Jul 27. PubMed PMID: 21795621; PubMed Central PMCID: PMC3214092.

Tabakoff B, Nelson E, Yoshimura M, Hellevuo K, Hoffman PL. Phosphorylation cascades control the actions of ethanol on cell cAMP signalling. J Biomed Sci. 2001 Jan-Feb;8(1):44-51. doi: 10.1007/BF02255970. Review. PubMed PMID: 11173975.

Tateno T, Robinson HP. The mechanism of ethanol action on midbrain dopaminergic neuron firing: a dynamic-clamp study of the role of I(h) and GABAergic synaptic integration. J Neurophysiol. 2011 Oct;106(4):1901-22. doi: 10.1152/jn.00162.2011. Epub 2011 Jun 22. PubMed PMID: 21697445.

Tu Y, Kroener S, Abernathy K, Lapish C, Seamans J, Chandler LJ, Woodward JJ. Ethanol inhibits persistent activity in prefrontal cortical neurons. J Neurosci. 2007 Apr 25;27(17):4765-75. doi: 10.1523/JNEUROSCI.5378-06.2007. PubMed PMID: 17460089; PubMed Central PMCID: PMC3625968.

Van Skike CE, Goodlett C, Matthews DB. Acute alcohol and cognition: Remembering what it causes us to forget. Alcohol. 2019 Sep;79:105-125. doi: 10.1016/j.alcohol.2019.03.006. Epub 2019 Apr 11. Review. PubMed PMID: 30981807.

Wahl-Schott C, Biel M. HCN channels: structure, cellular regulation and physiological function. Cell Mol Life Sci. 2009 Feb;66(3):470-94. doi: 10.1007/s00018-008-8525-0. Review. PubMed PMID: 18953682.

Wakita M, Shin MC, Iwata S, Nonaka K, Akaike N. Effects of ethanol on GABA(A) receptors in GABAergic and glutamatergic presynaptic nerve terminals. J Pharmacol Exp Ther. 2012 Jun;341(3):809-19. doi: 10.1124/jpet.111.189126. Epub 2012 Mar 20. PubMed PMID: 22434676.

Yan H, Li Q, Fleming R, Madison RD, Wilson WA, Swartzwelder HS. Developmental sensitivity of hippocampal interneurons to ethanol: involvement of the hyperpolarization-activated current, Ih. J Neurophysiol. 2009 Jan;101(1):67-83. doi: 10.1152/jn.90557.2008. Epub 2008 Oct 29. PubMed PMID: 18971298; PubMed Central PMCID: PMC2637011.

Zhang XX, Min XC, Xu XL, Zheng M, Guo LJ. ZD7288, a selective hyperpolarization-activated cyclic nucleotide-gated channel blocker, inhibits hippocampal synaptic plasticity. Neural Regen

Res. 2016 May;11(5):779-86. doi: 10.4103/1673-5374.182705. PubMed PMID: 27335562; PubMed Central PMCID: PMC4904469.

Zorumski CF, Mennerick S, Izumi Y. Acute and chronic effects of ethanol on learning-related synaptic plasticity. Alcohol. 2014 Feb;48(1):1-17. doi: 10.1016/j.alcohol.2013.09.045. Epub 2013 Dec 16. Review. PubMed PMID: 24447472; PubMed Central PMCID: PMC3923188.

Figure captions

Figure 1. Neurophysiological and pharmacological properties of HCN-mediated I_h recorded in rat CA3 pyramidal neurons. (A) Representative traces of I_h evoked in response to 2-s steps of increasing membrane hyperpolarization from the holding potential of -40 mV to -120 mV. **(B)** Activation curve of I_h. The data, derived from experiments as in (A), are expressed as I_h amplitude normalized for cell capacitance, and are averaged from 4 different neurons ± SEM. **(C)** Representative I_h traces evoked by the fully activated protocol applied to a single neuron. The open channel *I-V* curve is obtained by first hyperpolarizing the cell membrane to -120 mV for 2 s, to fully activate I_h, and subsequently setting the holding potential to the different test potentials (from -120 to -40 mV). **(D)** The fully activated I_h *I-V* curve, as in (C), was used to extrapolate the reversal potential, indicated by the arrow. **(E)** Representative traces showing the inhibitory effects of CsCl (5 mM) and the selective HCN blocker ZD7288 (20 μM) on I_h. The protocol of stimulation is indicated below the traces in the middle.

Figure 2. Concentration-dependent effects of EtOH on I_h recorded in rat CA3 pyramidal neurons. (A) Bar graph summarizing the changes in I_h amplitude produced by different concentrations of EtOH (10 - 80 mM) bath-perfused for 10 min. Data are expressed as the mean percent of baseline ± SEM. **(B)** Representative traces showing the effects of 20 and 80 mM EtOH on the amplitude of I_h evoked by a hyperpolarizing step to – 115 mV. **(C)** The scatter graph illustrates

the distribution of individual values relative to the effects of 20 and 80 mM EtOH, as in (A). **(D)** The graph shows the time-dependent effect of the bath-perfusion of 80 mM EtOH on I_h amplitude and its reversal during washout. **(E)** Effects of 20 and 80 mM EtOH on I_h rise time. Data are expressed as mean percent of baseline ± SEM. **(F-G)** Effects of 20 and 80 mM EtOH on the I_h activation curve (F) and fully activated I_h *I-V* curve (G). **(H)** Bar graph summarizing the effects of 20 and 80 mM EtOH in the absence and presence of the HCN antagonist ZD7288 (20 µM). The number of cells analyzed is indicated in each bar. **P* < 0.05, ***P* < 0.01, ****P* < 0.001 vs. baseline.

Figure 3. Effects of EtOH on temporal summation of evoked postsynaptic potentials recorded in hippocampal CA3 pyramidal neurons. Representative traces of evoked dendritic EPSP in the presence of ZD7288 (20 µM) **(A)**, EtOH (20 mM) **(C)**, and EtOH (80 mM) **(E)**. **B, D, and F** show the relative scatter plots of the quantitative effects of ZD7288 and EtOH on temporal summation. Data are expressed as ratio between EPSP4 and EPSP1. **P* < 0.05, ***P* < 0.001 vs. control (n = 3 – 9 cells).

Figure 4. EtOH and ZD7288 modulation of K^+-evoked firing activity in hippocampal CA3 pyramidal neurons. **(A)** Sample traces show the effect of the perfusion with ACSF containing 10 mM KCl (control), 20 µM bicuculline, and 1 mM kynurenic acid, on firing rate of CA3 pyramidal neurons in the cell-attached configuration, and subsequently the changes produced by ZD7288 (20 µM), EtOH (20 mM), and EtOH (80 mM). **(B)** and **(C)** Time-course of the effects of ZD7288 and the two concentrations of EtOH on K^+-evoked firing rate. Data are expressed as percent change from control. (n = 3 – 5 cells).

Figure 5. Dopamine enhances I_h amplitude in CA3 pyramidal neurons. (A) Representative traces of I_h recorded at -115 mV during bath-perfusion of the adenylate cyclase inhibitor DDA (10 µM), dopamine (DA, 10 µM), and the co-application of DA with the selective D1 receptor antagonist

SCH23390 (5 μM), or DDA. **(B)** The graph illustrates the time-dependent changes in I_h amplitude in the presence of the different drugs. DDA or SCH23390 were pre-incubated for 15 min before the co-application with DA for further 5 min. Data are expressed as mean percent of the baseline value ± SEM (n = 3-10). *$P < 0.01$.

Figure 6. Modulation of I_h amplitude by forskolin in CA pyramidal neurons. (A) Representative traces of I_h in the absence and presence of 0.1 and 30 μM forskolin. **(B)** Bar graphs showing the dose-dependent effects of forskolin on I_h modulation; data are expressed as mean percent of the baseline value ± SEM. **(C)** Representative traces of I_h illustrating the effects of the PKA inhibitor H89 on 0.1 and 30 μM forskolin. **(D)** Bar graph summarizing the effects of the two concentrations of forskolin in the absence and presence of H89. The number of cells analyzed is indicated in each bar. *$P < 0.05$ vs. baseline; #$P < 0.001$.

Figure 7. The biphasic modulation of I_h by EtOH is blocked by DDA and H89. Representative traces showing the effects of DDA and H89 on the modulatory action exerted by 20 mM EtOH **(A)** and 80 mM EtOH **(B)** on I_h amplitude. **(C)** Bar graph summarizing the effects of 20 and 80 mM EtOH in the absence or presence of DDA and H89. The number of cells analyzed is indicated in each bar. *$P < 0.05$; **$P < 0.01$ vs. control.

Figure 1

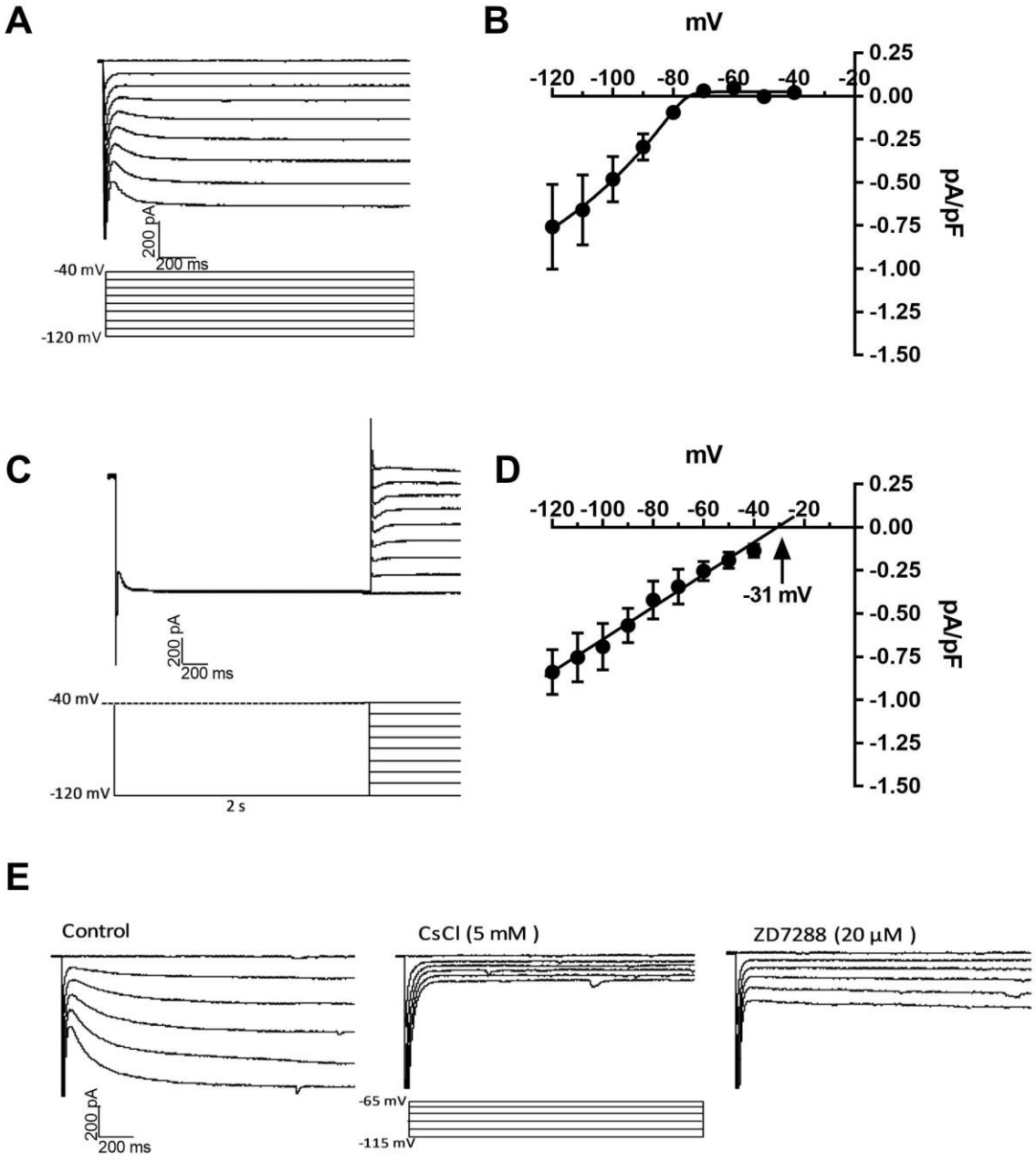
A
200 pA
200 ms
-40 mV
-120 mV
B
mV
-120 -100 -80 -60 -40 -20
0.25
0.00
-0.25
-0.50
-0.75
-1.00
-1.25
-1.50
pA/pF
C
200 pA
200 ms
-40 mV
-120 mV
2 s
D
mV
-120 -100 -80 -60 -40 -20
-31 mV
0.25
0.00
-0.25
-0.50
-0.75
-1.00
-1.25
-1.50
pA/pF
E
Control
CsCl (5 mM)
ZD7288 (20 µM)
200 pA
200 ms
-65 mV
-115 mV

757

Figure 2

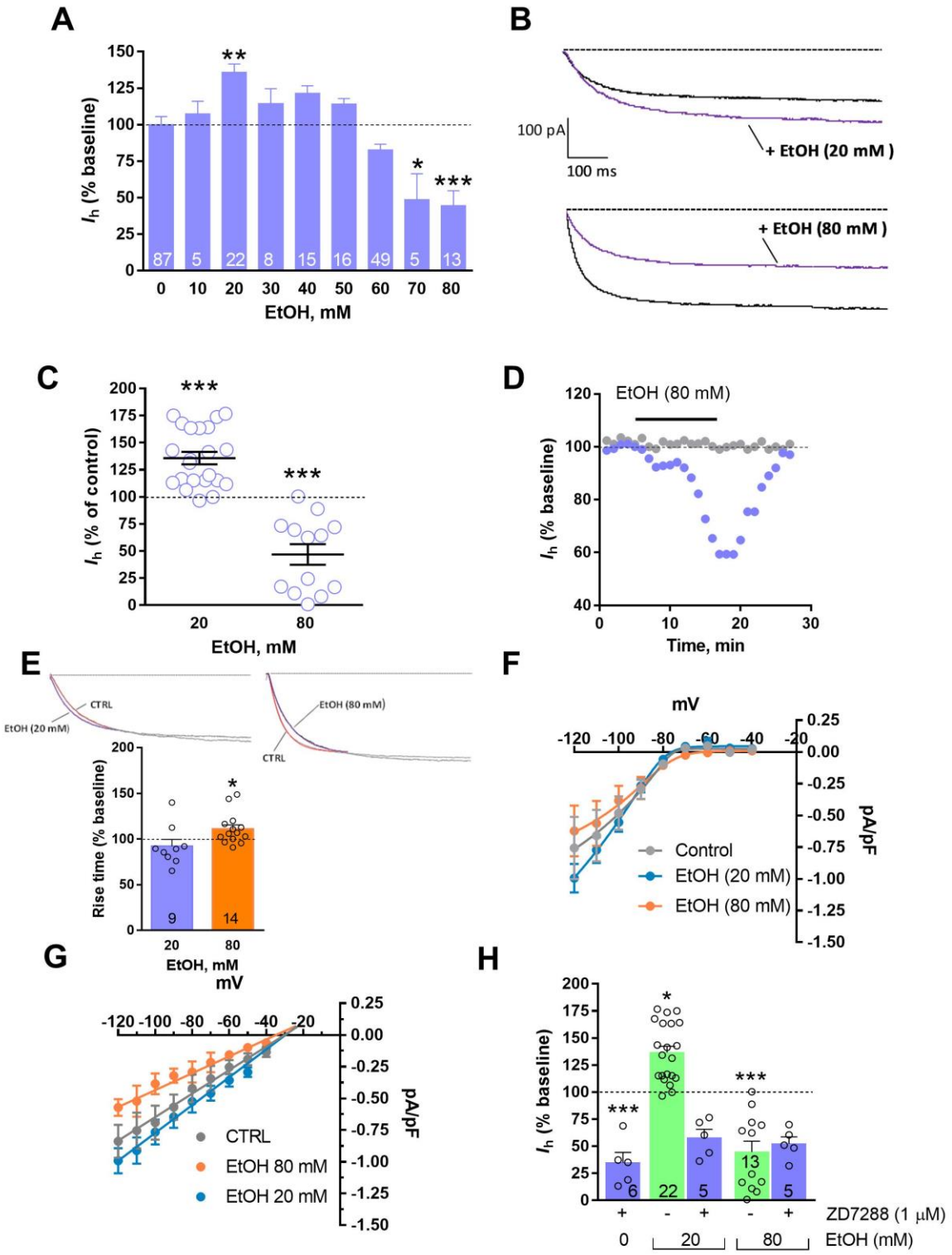
A
B
C
D
E
F
G
H
I_h (% baseline)
EtOH, mM
100 pA
100 ms
+ EtOH (20 mM)
+ EtOH (80 mM)
I_h (% of control)
EtOH (80 mM)
Time, min
CTRL
EtOH (20 mM)
Rise time (% baseline)
mV
pA/pF
Control
EtOH (20 mM)
EtOH (80 mM)
CTRL
EtOH 80 mM
EtOH 20 mM
ZD7288 (1 μM)
EtOH (mM)

758

Figure 3

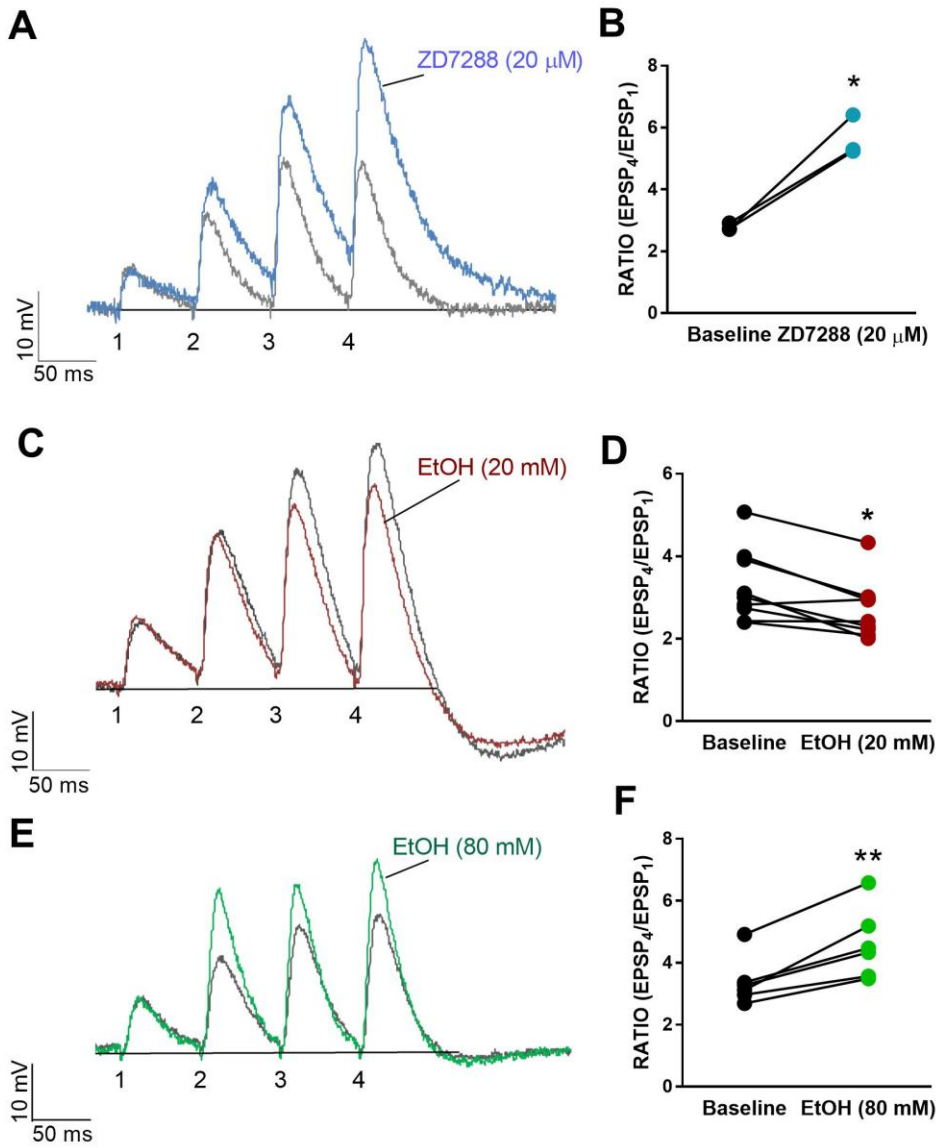
A
ZD7288 (20 μM)
10 mV
50 ms
1
2
3
4
B
RATIO (EPSP4/EPSP1)
Baseline ZD7288 (20 μM)
*
C
EtOH (20 mM)
D
Baseline EtOH (20 mM)
E
EtOH (80 mM)
F
Baseline EtOH (80 mM)
**

Figure 4

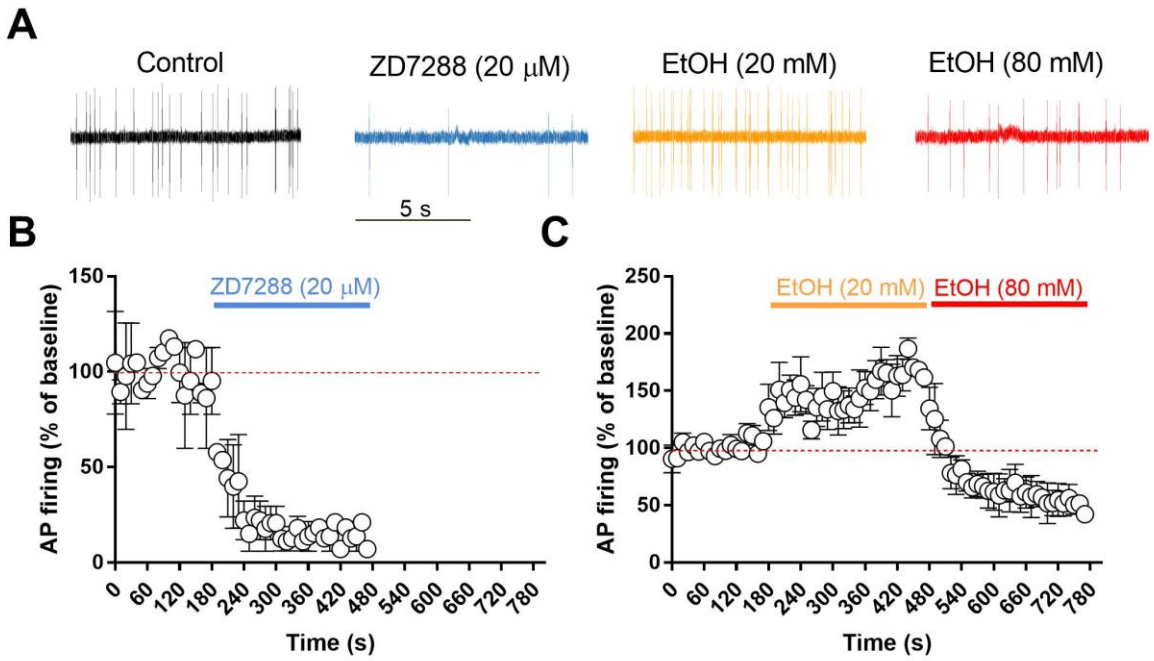
A
Control
ZD7288 (20 μM)
EtOH (20 mM)
EtOH (80 mM)
5 s
B
ZD7288 (20 μM)
AP firing (% of baseline)
Time (s)
C
EtOH (20 mM)
EtOH (80 mM)
AP firing (% of baseline)
Time (s)

Figure 5

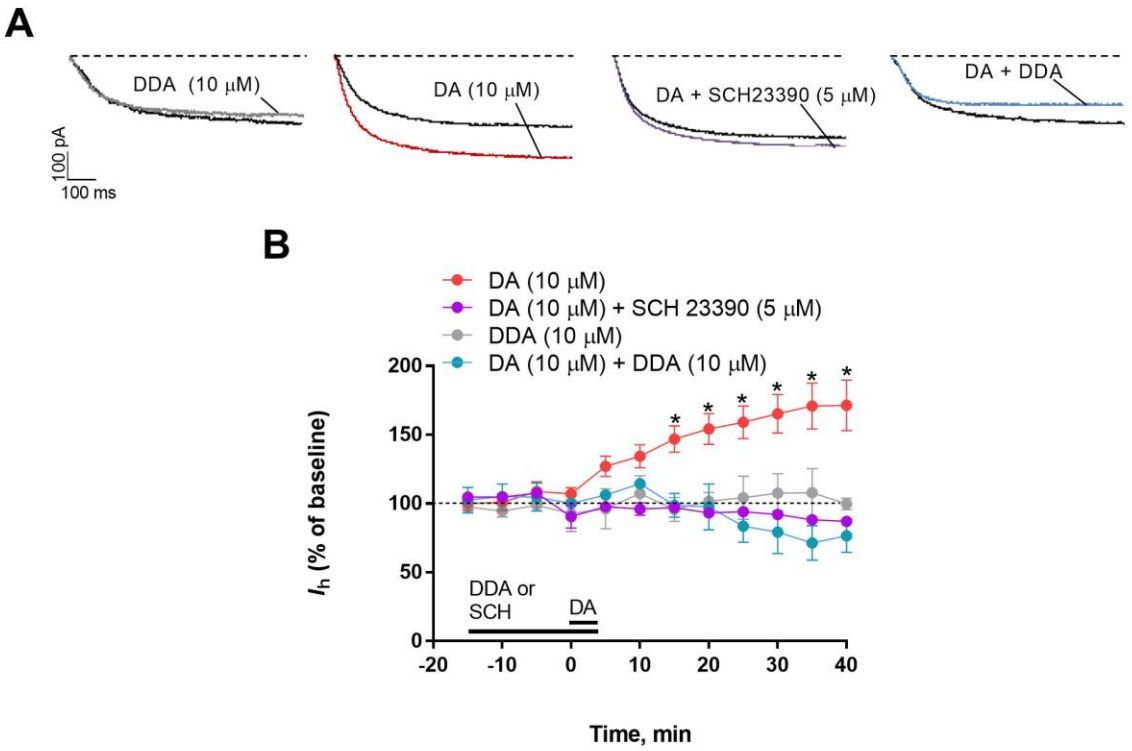
A
DDA (10 μM)
DA (10 μM)
DA + SCH23390 (5 μM)
DA + DDA
100 pA
100 ms
B
DA (10 μM)
DA (10 μM) + SCH 23390 (5 μM)
DDA (10 μM)
DA (10 μM) + DDA (10 μM)
I_h (% of baseline)
200
150
100
50
0
DDA or SCH
DA
-20
-10
0
10
20
30
40
Time, min

761

Figure 6

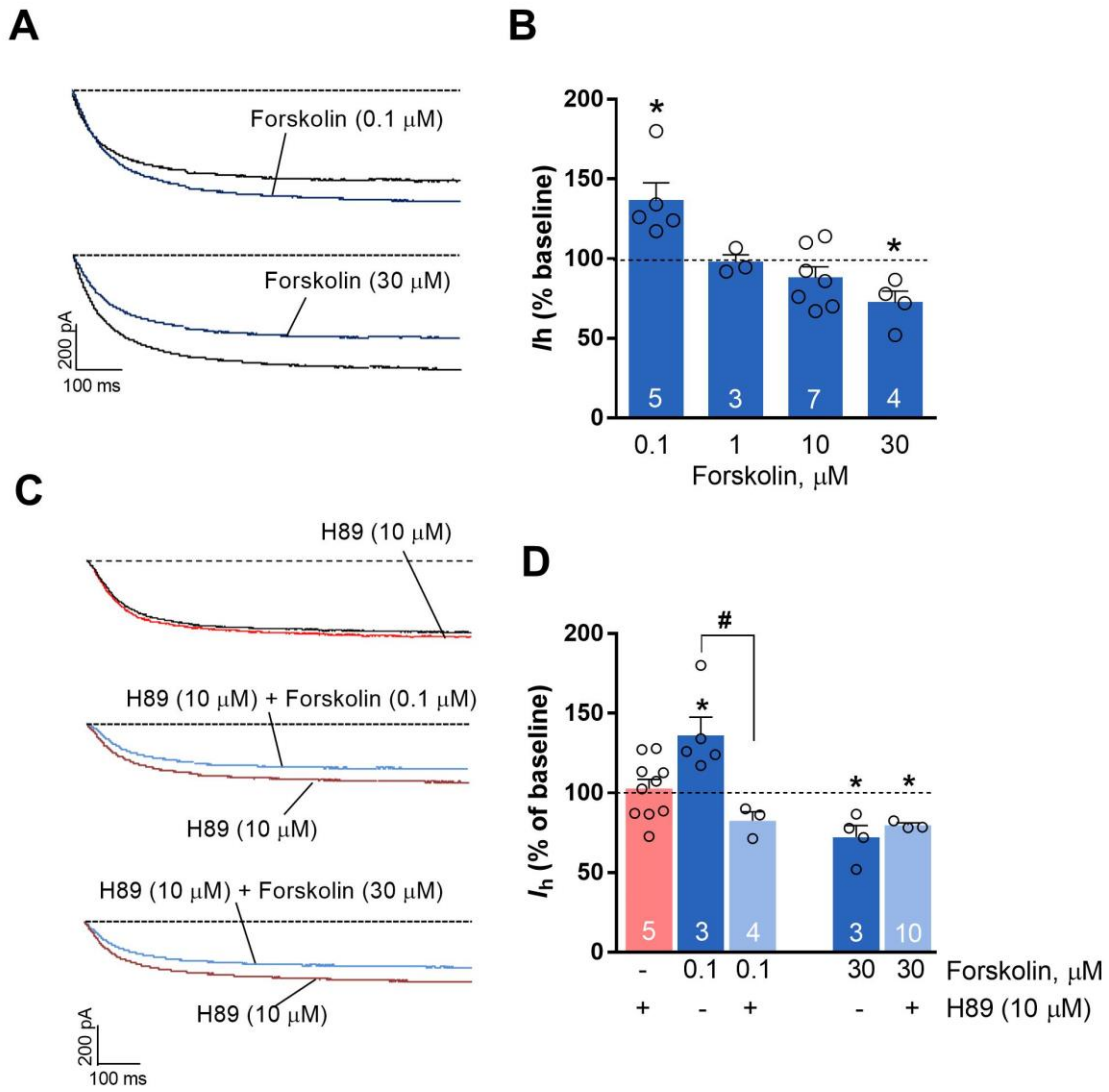
A
Forskolin (0.1 μM)
Forskolin (30 μM)
200 pA
100 ms
B
Ih (% baseline)
200
150
100
50
0
5
3
7
4
0.1
1
10
30
Forskolin, μM
C
H89 (10 μM)
H89 (10 μM) + Forskolin (0.1 μM)
H89 (10 μM)
H89 (10 μM) + Forskolin (30 μM)
H89 (10 μM)
200 pA
100 ms
D
Ih (% of baseline)
200
150
100
50
0
#
5
3
4
3
10
-
0.1
0.1
30
30
Forskolin, μM
+
-
+
-
+
H89 (10 μM)

Figure 7

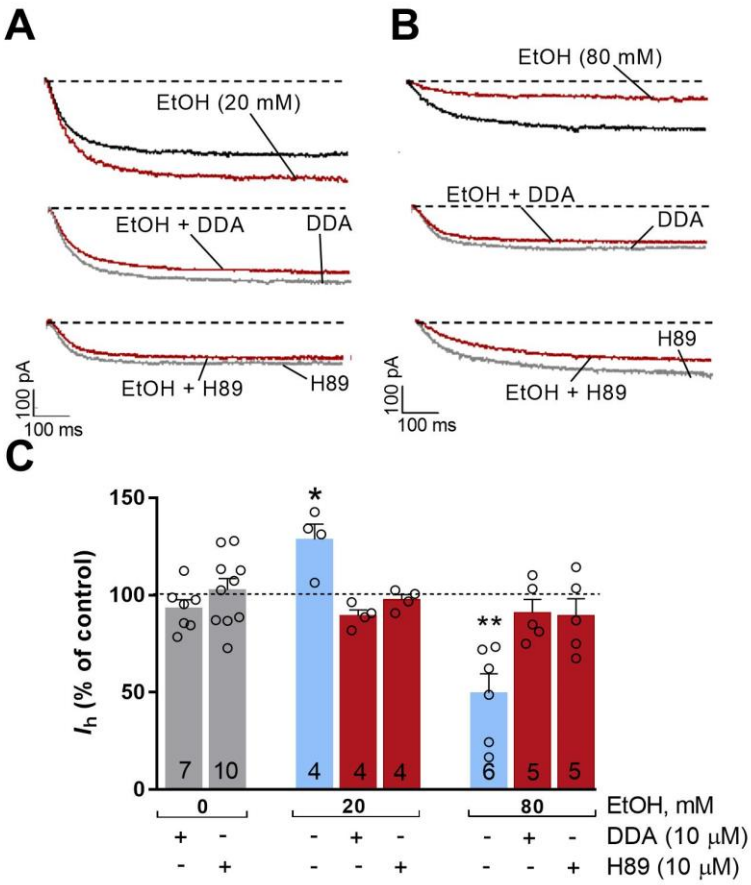
A
EtOH (20 mM)
EtOH + DDA
DDA
EtOH + H89
H89
100 pA
100 ms
B
EtOH (80 mM)
EtOH + DDA
DDA
H89
EtOH + H89
100 pA
100 ms
C
I_h (% of control)
150
100
50
0
*
**
7
10
4
4
4
6
5
5
0
20
80
EtOH, mM
DDA (10 μM)
H89 (10 μM)